

This article was downloaded by: [Kansas State University Libraries]

On: 17 May 2010

Access details: Access Details: [subscription number 768172861]

Publisher Taylor & Francis

Informa Ltd Registered in England and Wales Registered Number: 1072954 Registered office: Mortimer House, 37-41 Mortimer Street, London W1T 3JH, UK



Aerosol Science and Technology

Publication details, including instructions for authors and subscription information:

<http://www.informaworld.com/smpp/title~content=t713656376>

Aerosol Gelation: Synthesis of a Novel, Lightweight, High Specific Surface Area Material

Rajan Dhaubhadel ^a; Corey S. Gerving ^a; Amitabha Chakrabarti ^a; Christopher M. Sorensen ^a

^a Department of Physics, Kansas State University, Manhattan, Kansas, USA

First published on: 01 August 2007

To cite this Article Dhaubhadel, Rajan , Gerving, Corey S. , Chakrabarti, Amitabha and Sorensen, Christopher M. (2007) 'Aerosol Gelation: Synthesis of a Novel, Lightweight, High Specific Surface Area Material', *Aerosol Science and Technology*, 41: 8, 804 — 810, First published on: 01 August 2007 (iFirst)

To link to this Article: DOI: 10.1080/02786820701466291

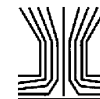
URL: <http://dx.doi.org/10.1080/02786820701466291>

PLEASE SCROLL DOWN FOR ARTICLE

Full terms and conditions of use: <http://www.informaworld.com/terms-and-conditions-of-access.pdf>

This article may be used for research, teaching and private study purposes. Any substantial or systematic reproduction, re-distribution, re-selling, loan or sub-licensing, systematic supply or distribution in any form to anyone is expressly forbidden.

The publisher does not give any warranty express or implied or make any representation that the contents will be complete or accurate or up to date. The accuracy of any instructions, formulae and drug doses should be independently verified with primary sources. The publisher shall not be liable for any loss, actions, claims, proceedings, demand or costs or damages whatsoever or howsoever caused arising directly or indirectly in connection with or arising out of the use of this material.



Aerosol Gelation: Synthesis of a Novel, Lightweight, High Specific Surface Area Material

Rajan Dhaubhadel, Corey S. Gerving, Amitabha Chakrabarti,
 and Christopher M. Sorensen

Department of Physics, Kansas State University, Manhattan, Kansas, USA

We demonstrate that an aerosol can gel. This gelation is then used for a one-step method to produce an ultralow density porous carbon material. This material is named an aerosol gel because it is made via gelation of particles in the aerosol phase. The carbon aerosol gels have high specific surface area (200–350 m²/g), an extremely low density (2.5–5.0 mg/cc) and a high electrical conductivity, properties similar to conventional aerogels. The primary particles of the carbon aerosol gels are highly crystalline with a narrow (002) graphitic X-ray diffraction peak. Key aspects to form a gel from an aerosol are large volume fraction, ca. 10^{−4} or greater, and small primary particle size, 50 nm or smaller, so that the gel time is fast compared to other characteristic times.

1. INTRODUCTION

We report a novel one-step method to produce porous materials via the gelation of nanoparticles in the aerosol phase. We have named these materials *aerosol gels*. Here we describe carbon aerosol gels made via carbon nanoparticle gelation. However, our work indicates that any collection of finely divided primary particles with large enough volume fraction can produce an aerosol gel when allowed to aggregate regardless of the chemical composition of the parent primary particles. In the case of the carbon aerosol gel the initial aerosol is composed of nanometer sized carbon particles produced rapidly by exploding any one of a number of hydrocarbons with oxygen in a closed chamber. These nanometer sized carbon particles quickly aggregate and then gel to form the aerosol gel (Dhaubhadel et al. 2006). Unlike conventional aerogels this method of making an aerosol gel is not a wet process and does not require a catalyst. The carbon aerosol gels have properties comparable to those of the carbon

aerogels obtained by pyrolyzing sol-gel synthesized resorcinol-formaldehyde aerogels in an inert atmosphere (Reynolds et al. 1996; Pekala et al. 1994). This carbon aerosol gel is significantly different from ordinary carbon black and soot formed as byproducts during combustion of any hydrocarbon fuel; it is a new material.

2. AEROSOL GELATION

A form of aerosol gelation was first reported by Lushnikov and coworkers (Lushnikov et al. 1990). The gel formed in the presence of an electric field which enhanced aggregation of solid particles along field lines. Subsequently our laboratory has reported gelation of soot in laminar diffusion flames (Sorensen et al. 1998; Kim et al. 2006). Simulations (Gimel et al. 1995, 1999; Hasmy and Jullien 1996; Fry et al. 2004) imply that any system of particles undergoing aggregation can form a gel if the combining particles do not coalesce, and if the time to reach the gel point is shorter than other time scales that can deter gel formation. Non-coalescence is necessary so that the aggregating particles will form a non-dense (ramified) fractal aggregate with fractal dimension, D , less than the spatial dimension, d . When $D < d$, the average cluster separation to cluster size ratio falls with time during aggregation until the separation equals the size. Then the clusters jam together to form a gel.

A reasonable approximation for when the particulate system gels is when the monomer or primary particle number density in the average cluster $n_{cluster}$ is equal to the primary particle number density in the entire system n_{system} , i.e.,

$$n_{cluster} = n_{system} \quad [1]$$

For a fractal aggregate (cluster) the number of primary particles N of radius a in a cluster of radius R is approximately

$$N \approx (R/a)^D. \quad [2]$$

Then the primary particle number density in the cluster in three-dimensional space is

$$n_{cluster} \approx N/R^3 = R^{D-3}/a^D. \quad [3]$$

Received 22 August 2006; accepted 22 May 2007.

We thank Prof. Kenneth J. Klabunde for use of his BET instrument and also thank Dr. Daniel L. Boyle for TEM work. This research was supported by NASA Grant No. NNC04GA74G and NSF Grant No. CTS 0080017.

Address correspondence to Christopher M. Sorensen, Department of Physics, Kansas State University, Manhattan, Kansas 66506, USA. E-mail: sor@phys.ksu.edu

The system primary particle number density is related to the particulate volume fraction f_v by

$$f_v \approx n_{\text{system}} a^3. \quad [4]$$

Then Equations (1), (3), and (4) yield the size of the cluster at the gel point

$$R_{\text{gel}} \approx a f_v^{\frac{1}{D-3}}. \quad [5]$$

For Diffusion Limited Cluster Aggregation (DLCA) $D = 1.8$ this is

$$R_{\text{gel}} \approx a f_v^{-5/6}. \quad [6]$$

The gel time is the time for a cluster to grow to R_{gel} . Kinetics of growth are governed by the Smoluchowski Equation which in its simplest form is

$$\frac{dn_c}{dt} = -K n_c^2. \quad [7]$$

In Equation (7) n_c is the number density of clusters and K is the aggregation constant. The long time solution to Equation (7) is

$$n_c(t) \approx (Kt)^{-1}. \quad [8]$$

The cluster and primary particle number densities are related by

$$n_{\text{system}} = N n_c. \quad [9]$$

n_{system} is a constant and N and n_c vary with time. The gel time can be found by setting the number of primary particles per cluster N to its value at the gel point through Equations (2) and (5) as

$$N_{\text{gel}} \approx f_v^{D/(D-3)}. \quad [10]$$

Then combining Equations (4), (8), (9), and (10) one can find the gel time

$$t_{\text{gel}} \approx K^{-1} a^3 f_v^{-3/(3-D)}. \quad [11]$$

For $D = 1.8$ Equation (11) becomes

$$t_{\text{gel}} \approx K^{-1} a^3 f_v^{-2.5}. \quad [12]$$

Equation (12) was derived under the assumptions of spherical clusters, all the same size, with no interpenetration. Despite these caveats, it has the important implication that if a is small and f_v is large, i.e., if there is a lot of finely divided matter, the system will gel fast. Moreover, the functionalities on a and f_v are very strong. Equation (12) is plotted in Figure 1. For the aggregation constant K the value for air at STP is used, $K = 3 \times 10^{-10} \text{ cm}^3/\text{s}$. Figure 1 shows that an aerosol can gel quickly, 100 s or less, if $a \sim 10 \text{ nm}$

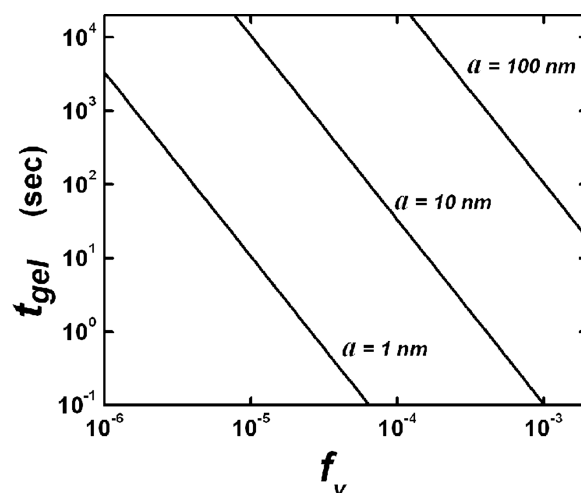


FIG. 1. Functionalities of the gel time.

and $f_v \sim 10^{-4}$. Coarser aerosols at lower f_v have huge gel times and essentially never gel because other factors, e.g., gravitational setting, occur first. The condition in our chamber are different than this simple example so the details of the gel times will be different, but the important lesson is that aerosols can be made with gel times short enough to be experimentally obtainable.

The conditions for rapid gel formation, $f_v \geq 10^{-4}$ and $a \sim 10 \text{ nm}$, can be obtained with rapid, gas phase reaction. Any gas at STP if converted directly to a solid will yield a solid f_v of about 10^{-3} (recall that gases are about 1,000 times less dense than the condensed phase). Rapid reactions from the gas to the solid phase will drive the system deep into a supersaturated regime. Thus rapid and uniform nucleation to small particles will occur. This is what we did to form carbon aerosol gels.

3. EXPERIMENTAL METHODS

The carbon aerosol gel was made by exploding a mixture of a hydrocarbon and oxygen in a chamber at one atmosphere pressure. Introducing an electric spark triggered the explosion. The explosion was carried out in two different aluminum cylindrical chambers with different sizes. The larger chamber had a volume of 16.6 liters; the smaller a volume of 3.9 liters. Results were chamber independent.

Methane (CH_4), acetylene (C_2H_2), ethylene (C_2H_4), and propane (C_3H_8) were used as gaseous hydrocarbon fuels. Liquid hydrocarbons used were butane (C_4H_{10}), pentane (C_5H_{12}), hexane (C_6H_{14}), and isooctane (C_8H_{18}). Butane has highest vapor pressure (1557 mm of Hg at 20°C) and lowest boiling point (-0.5°C), so vaporizes instantly and can be exploded like other gaseous hydrocarbons. Pentane and hexane have vapor pressures of 433 and 131 mm of Hg at 20°C , respectively, and boiling points 36 and 68.7°C , respectively. Thus they can be easily vaporized by increasing the temperature slightly and waiting for few minutes, and then can be exploded easily inside the chamber. Isooctane has lowest vapor pressure 41 mm of Hg at 20°C and highest boiling point 99°C and thus is a little harder to deal with.

To explode, aerosols of isooctane microdroplets were first prepared by using an ultrasonic nebulizer, which were then sprayed into the chamber filled with oxygen.

There are minimum and maximum limits called Lower Explosion Limit (LEL) and Higher Explosion Limit (HEL) for the mixing proportion of a hydrocarbon fuel and oxygen in order to explode. Material Safety Data Sheet (MSDS) lists the LEL and HEL in terms of the percentage of the fuel in a fuel–air mixture (MSDS 1970). These LEL and HEL were recalculated to account for a pure oxygen environment and used to prepare the mixture ready for explosion in the chambers.

4. RESULTS AND DISCUSSION

The chamber was opened several minutes after exploding the fuel–oxygen mixture to obtain a dark black fluffy carbon layer (Figure 2) on the bottom and some lumps here and there clinging on the walls and ceiling of the chamber for all fuels except methane and butane which did not yield a soot. This layer on the bottom was about 2 cm thick for acetylene and ≤ 3 mm for other hydrocarbon fuels in 16.6 liter chamber. These results seem to imply that the aerosol gel was a result of sedimentation and wall deposition and not the gelation process.

When the chamber was opened within a minute or less after the explosion, however, we observed that it was completely filled with a very delicate aerosol gel which usually collapsed, like a “falling” cake, to yield the deposits on the bottom and walls. Sometimes when the chamber was opened after the explosion, the air convection from the removal of the lid caused chunks of aerosol gel several centimeters in size to fly out of the chamber. A series of top view pictures in Figure 3 demonstrates the gravitationally collapsing aerosol gel network from acetylene in the chamber. Picture (a), taken 2 minutes after creating the aerosol and 5 seconds after opening the lid, shows the gel filled almost to the top of the 24 cm wide 37 cm deep chamber.

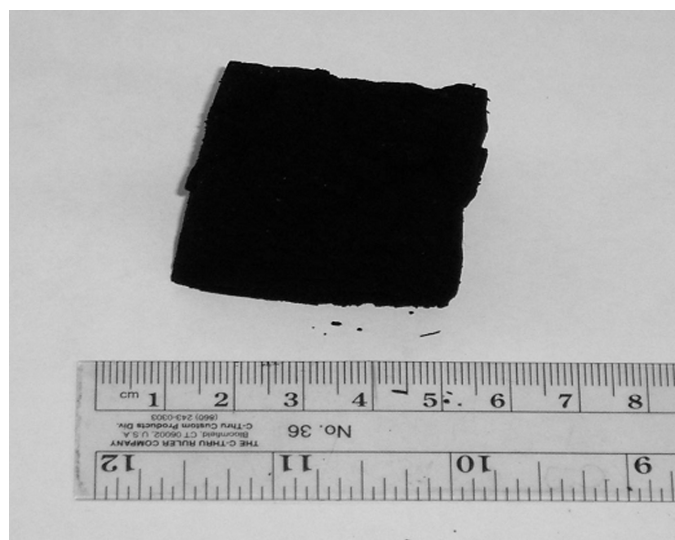


FIG. 2. Carbon aerosol gel, density = 2.5 mg/cc.

The aerosol gel collapsed somewhat 30 sec after the lid was opened (Picture (b)). Picture (c) indicates that the gel collapsed by more than half the depth of the chamber 1 min after opening the lid. Further collapsing was relatively slow. Pictures (d) and (e) were taken 1.5 min and 2 min, respectively, after opening the chamber. Finally, picture (f) taken 20 min after the chamber was opened shows a completely collapsed gel to about 2 cm thick layer on the bottom of the chamber.

These pictures graphically demonstrate that a macroscopic, three dimensional gel can form from the aggregation of an aerosol. During the aggregation, the mean cluster size of the aerosol has grown from the monomer size of about 50 nm to the container size of nearly 0.5 meter, a change of seven orders of magnitude!

In other work we used a thin cylindrical disc chamber with circular glass windows on both ends of the cylinder. The internal space of the chamber was 51 mm diameter wide and 10 mm thick. This chamber was used for light scattering studies from the gelling aerosol reported elsewhere. After acetylene gas was exploded in this chamber, we initially observed an unresolved aerosol that coarsened with time until a volume spanning gel network formed within ca. 100 seconds.

From a broad perspective this aerosol gel we collect from the bottom and walls of the chamber was a result of an aerosol gelation process likely involving Brownian motion during the major growth period, then convection, wall deposition and gravitational settling.

With success in producing the aerosol gels from different liquid and gaseous hydrocarbon fuels we concentrated mostly on detail studies of the aerosol gel from acetylene and some other gaseous hydrocarbons.

Density Measurement

The density of the carbon aerosol gel was determined by measuring the mass of a known volume of the sample using an electronic balance with sensitivity of 1 mg. Table 1

TABLE 1
Aerosol gel densities for numerous synthesis runs obtained for selected fuels

Hydrocarbon Fuels	Density		
	Lowest (mg/cc)	Highest (mg/cc)	Average (mg/cc)
Gaseous Fuels			
Acetylene	3.5	6.5	5.0
Ethylene	2.3	3.5	2.9
Propane	2.1	3.3	2.7
Liquid Fuels			
Pentane	2.4	8.6	5.1
Hexane	4.7	5.4	4.9
Isooctane	2.3	11.2	5.8

Pure Graphite has density of 2.25 g/cc.

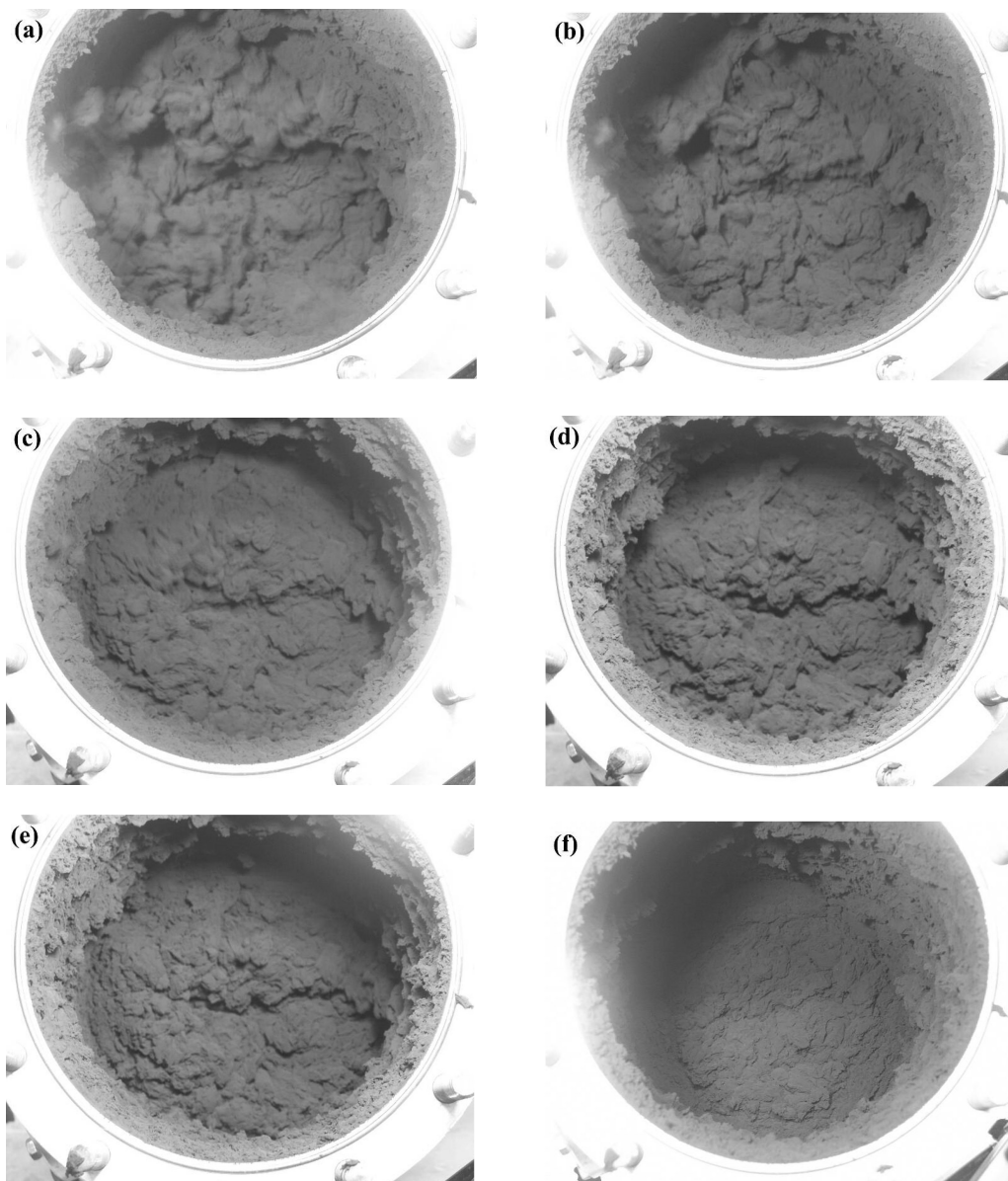


FIG. 3. A series of top view pictures of gravitationally collapsing acetylene aerosol gel in the 24 cm wide 37 cm deep chamber. (a) The gel was found to fill almost to the top 2 minutes after creating the aerosol and 5 seconds after opening the lid. (b) The aerosol gel collapsed somewhat 30 sec after the lid was opened. (c) The gel collapsed by more than half the depth of the chamber 1 min later. Relatively slow collapsing was observed afterwards. (d) 1.5 min later. (e) 2 min later. (f) Gel collapsed completely to about a 2 cm thick layer 20 min later.

lists the densities of the carbon aerosol gels produced from the various hydrocarbons. The aerosol gel density is measured as low as 2.0 mg/cc, which is extraordinarily low. This density is less than twice the density of dry air at STP and is lower than any known solid or liquid material. The density measurements were qualitatively double checked by measuring the time taken by a roughly spherical aerosol gel to fall in air through a known height under the influence of gravity. Although the aerosol gel is delicate and fragile, it is still found capable to withstand a weight about 20 times itself without being crushed.

The aerosol gel was compressed by hand to examine the change in its density. Although the pressure involved in this process was unknown, the process was good enough to produce a homogeneous product for density measurement and to show how the specific surface area and electrical conductivity behave as a function of density (see subsections 4.2 and 4.4). The density was found to be about 300 mg/cc, an order of magnitude lower than graphite, even after grinding by hand in a mortar and pestle and then tightly compressing into a 5 cm long circular tube with 8 mm internal diameter. This shows that there are still voids preserved even after applying high pressures. The rigid bond

between the primary particles could be the reason for not being able to be close packed. It was noticed that the compressed aerosol gel expands back to some extent when the compressing force is removed showing elastic behavior.

Specific Surface Areas and Surface Porosity

The specific surface areas and surface porosity of the black carbon aerosol gels were determined using the Brunauer-Emmett-Teller (BET) analysis technique (Kruk et al. 2001) with nitrogen gas as an adsorbate. The results for both uncrushed and crushed samples are listed in Table 2. The acetylene and ethylene aerosol gels are found to have a high specific surface area of 350 m²/g while propane aerosol gel is found to have a lower specific surface area of 130 m²/g for uncrushed samples. If we assume the material density within a primary particle to be equal to that of graphite the BET results suggest an effective primary particle size, assumed to be spherical, of about $a = 10$ nm for propane aerosol gels and $a = 4$ nm for acetylene and ethylene aerosol gels, respectively. Acetylene aerosol gels are found to have a large specific mesopore volume of 0.56 cc/g for pores smaller than 135 nm diameter at relative pressure 0.986. The average pore diameter for this aerosol gel is measured to be 11.8 nm.

TABLE 2

Listing of the BET results averaged over different runs. The densities are about 10 mg/cc, higher than as prepared, due to some crushing during sample preparation

	Uncrushed Aerosol Gel		Crushed Aerosol Gel	
	Sample Density (mg/cc)	Specific Surface Area (m ² /g)	Sample Density (mg/cc)	Specific Surface Area (m ² /g)
Acetylene Aerosol Gel	10	350	160	150
Ethylene Aerosol Gel	10	350	50	200
Propane Aerosol Gel	10	130	100	100

Microscopic Structure of the Carbon Aerosol Gel

Figures 4(a), (b), and (c) show transmission electron microscopy (TEM) pictures for acetylene, ethylene, and propane aerosol gels, respectively. These pictures show that the aerosol gels are ramified fractal structures with pores trapped inside.

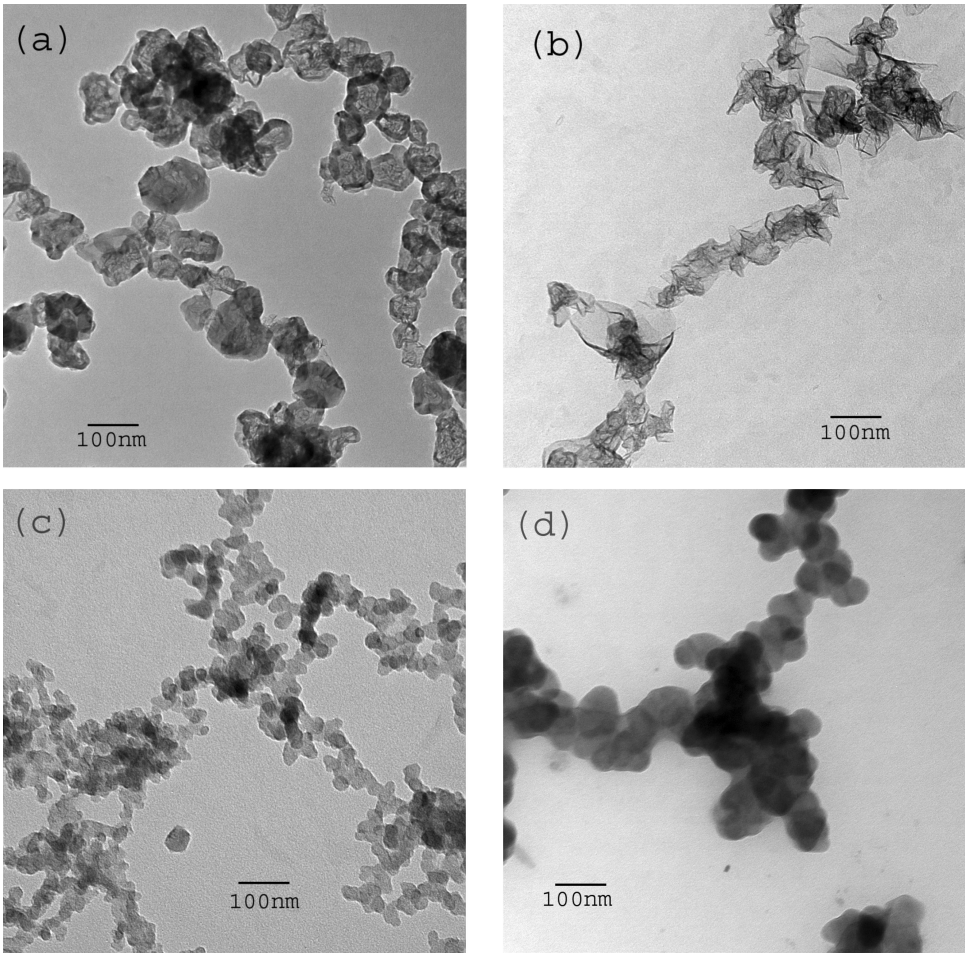


FIG. 4. TEM pictures of (a) an acetylene aerosol gel (b) an ethylene aerosol gel (c) a propane aerosol gel and (d) an acetylene open flame soot.

Primary particles with typical size $a = 38$ nm are found for both acetylene and ethylene aerosol gels. Propane aerosol gels have a smaller primary particle of typical size $a = 10$ nm. The primary particles of acetylene and propane aerosol gels are more or less polygonal in structure. In the Ethylene aerosol gel the primary particles are not well defined. Instead the structure looks like a thin ribbon with thick borders. From these TEM images it appears that the primary particles of the aerosol gels from acetylene and ethylene have graphitic layer planes a few nanometers thick around the surface with their planer orientation parallel to the particle surfaces forming a shell-like structure. What appears to be encapsulated inside this shell is either voids or amorphous carbon with more random crystallite orientation. These graphitic layer planes are quasi-crystalline and can be referred to as nanocrystals. In the case of the primary particles of the aerosol gel from propane the graphitic layer planes are not distinct.

The X-ray diffraction (XRD) patterns with distinct peaks also exhibit the crystalline property of the aerosol gel primary particles. Figure 5 shows the XRD patterns for the aerosol gels from acetylene, ethylene, and propane. This figure also includes the XRD pattern from an open flame acetylene soot for comparison purpose. An effective sizes of the nanocrystals were determined by Scherrer broadening (Cullity 1978), i.e., the size is inversely related to the angular width of the (002) diffraction peak. Among the three different aerosol gels investigated, propane aerosol gel has the broadest and acetylene aerosol gel has the narrowest diffraction peaks. From the Scherrer broadening measurement we found the crystallite size to be about 3 nm for acetylene and ethylene aerosol gels and about 2 nm for propane aerosol gel. A careful observation of

these XRD patterns also revealed the fact that the (002) peak shifts towards larger angle as we go from propane to acetylene aerosol gels. This indicates that the graphitic layer plane separation is largest for propane and smallest for acetylene aerosol gels. A range of lattice spacing within a soot monomer has been observed and reported in literature (Franklin 1950; Palotas et al. 1996a; Palotas et al. 1996b, 1998). These graphitic plane separations are found to be 3.59, 3.51, and 3.47 Å for propane, ethylene and acetylene aerosol gels respectively. The (101) peak observed in the XRD pattern however shifts towards smaller angle as we go from propane towards acetylene aerosol gels.

The primary particle sizes for acetylene and ethylene aerosol gels as measured from the TEM pictures are bigger compared with those determined from the BET and XRD results. This suggests that these primary particles are multicrystalline and porous. However the propane aerosol gel primary particles have sizes measured from TEM images and BET analysis approximately matching suggesting non-porosity. Monomeric particle sizes were measured with a reticle magnifier at roughly 10–20 locations in the TEM micrographs. This led us to monomer size measurements accurate to 10–20% which we warranted as good enough given the nonspherical, rather polygonal structure of the monomers. Indeed, in many cases the monomers seem to blend from one to the other. Given these morphological challenges, a more accurate determination with concomitant statistical analysis is not warranted. However, comparison to size scales inferred from BET, whatever these scales may be, is of value because they are much different in the cases of acetylene and ethylene precursors.

Thermal Gravimetric Analysis (TGA) showed that there is no significant change, less than 1% in the mass of the carbon aerosol gels, after heating from room temperature up to 600°C. This implied that there are no volatile substances present in the carbon aerosol gels.

The result from Energy Dispersive X-ray spectroscopy (EDS) shows only the peak due to the elemental carbon present in the aerosol gel revealing that it does not consist any other higher elemental composition.

Electrical Conductivity of the Carbon Aerosol Gel

The aerosol gel is found to be a good conductor of electricity with its conductivity increasing quadratically with increase in its density. This is unusual since most materials have a linear dependence. The aerosol gel was packed in a 8 mm internal diameter 5 cm long glass tube capped with brass terminals to measure the electrical conductivity. Figure 6 shows the conductivity versus density plot for acetylene aerosol gel. This plot also includes the conductivity for graphite (density 2250 mg/cc), which is $142.86 \Omega^{-1}\text{cm}^{-1}$. As is clear from the plot, the conductivity for the carbon soot with density 4.0 mg/cc is $2.86 \times 10^{-4} \Omega^{-1}\text{cm}^{-1}$, which is comparable to those of semiconductors.

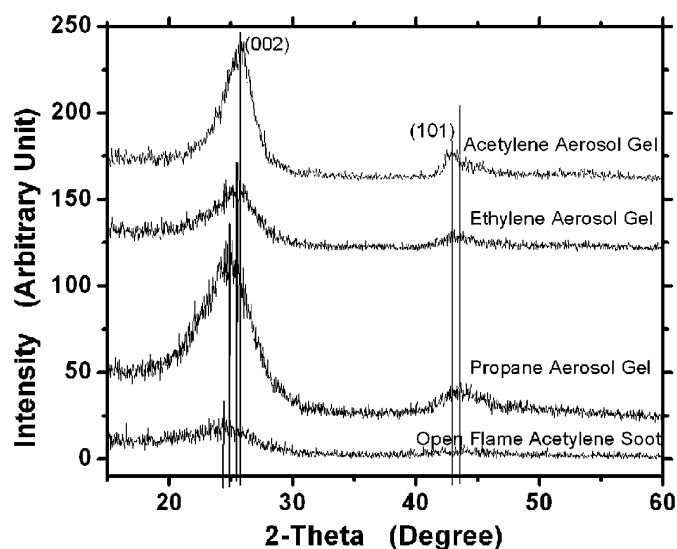


FIG. 5. X-ray diffraction of the compressed carbon aerosol gels and open flame acetylene soot. The vertical lines indicate the positions of the corresponding diffraction peaks.

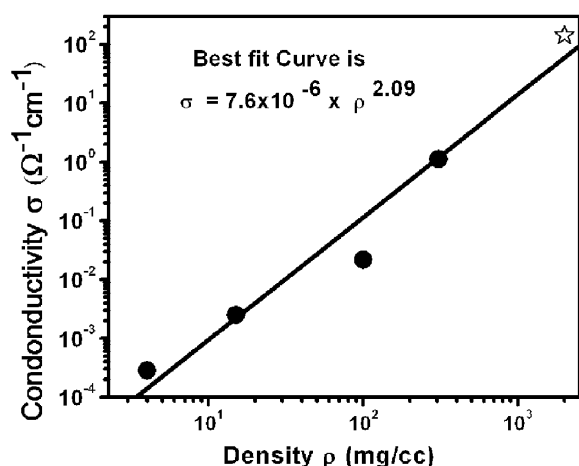


FIG. 6. Log-log plot of conductivity versus density at room temperature for acetylene aerosol gel. Quadratic variation of conductivity with density is observed. The data final point indicated by a star sign is for pure graphite.

Comparison with a Normal Open Flame Soot

The aerosol gel was compared with a normal open flame soot. The sample of an open flame soot was collected from an acetylene-air diffusion flame produced on a simple diffusion burner. The density of the open flame soot is found higher, ca. 13 mg/cc. Unlike the dark black aerosol gel, the open flame soot is dark gray in color. This indicates that the open flame soot might have contained hydrocarbons. A TEM comparison of the open flame soot shown in Figure 4(d) to the aerosol gel shown in Figures 4 (a), (b), and (c) shows that the open flame soot monomers are more rounded in shape and uniform, without a noticeable graphitic nature, unlike the graphitic polygonal shaped crystalline aerosol gel monomers. The XRD pattern for the open flame acetylene soot (Figure 5) shows a weak (002) and unnoticeable (101) peaks implying the amorphous nature unlike the aerosol gels. The position of (002) peak suggests the graphitic layer plane separation to be 3.66 nm, which is larger compare to those of the aerosol gels. The monomer diameter (2a) for an open flame soot is about 60 nm. The electrical conductivity of the open flame soot is found to be three orders of magnitude lower than that for the aerosol gel. However, two common characteristics were observed, i.e., both types of soot were hydrophobic and could be soaked with solvents like toluene. When crushed hard with a pestle, the aerosol gel became shiny showing its graphitic nature, but the open flame soot was still dull.

5. CONCLUSION

We have used a novel gelation of particles in the aerosols phase to create a new material that we have named aerosol gel. The nanoparticle aerosol was created by an explosion of a hydrocarbon/oxygen mixture. Aerosol gels have unusual properties including ultralow density and high specific surface area and

thus are similar to well-known aerogel materials. We believe the aerosol gels have advantages over conventional aerogels made via the sol-gel process (Brinker et al. 1990) in the sense that no supercritical drying step is required and thus complexities involved can be avoided. Though we have just produced carbon aerosol gels, our technique has the potential to lend itself to a wide class of materials, including those that have been developed into aerogels via the sol-gel process.

REFERENCES

- Brinker, C. J., and Scherer, G. W. (1990). *Sol-gel science*, Academic Press, San Diego.
- Cullity, B. D. (1978). *Elements of x-ray diffraction*, 2nd Edition, Addison-Wesley Publishing Company, Inc.
- Dhaubhadel, R., Pierce, F., Chakrabarti, A., and Sorensen, C. M. (2006). Hybrid Superaggregate Morphology as a Result of Aggregation in a Cluster-Dense Aerosol, *Phys. Rev. E* 73:011404-1.
- Franklin, Rosalind E. (1950). The Structure of Carbon, *Journal de Chimie Physique et de Physico-Chimie Biologique*. 47:573-575.
- Fry, D., Chakrabarti, A., Kim, W., and Sorensen, C. M. (2004). Structural Crossover in Dense Irreversibly Aggregating Particulate Systems, *Phys. Rev. E* 69:061401-10.
- Gimel, J. C., Durand, D., and Nicolai, T. (1995). Transition Between Flocculation and Percolation of a Diffusion-Limited Cluster-Cluster Aggregation Process Using Three-Dimensional Monte Carlo Simulation, *Phys. Rev. B* 51:11348-11357.
- Gimel, J. C., Nicolai, T., and Durand, D. (1999). 3D Monte Carlo Simulations of Diffusion Limited Cluster Aggregation Up to the Sol-Gel Transition: Structure and Kinetics, *J. Sol-Gel Sci. Technol.* 15:129-136.
- Hasmy, A. and Jullien, R. (1996). Percolation in Cluster-Cluster Aggregation Processes, *Phys. Rev. E* 53:1789-1794.
- Kim, W. G., Sorensen, C. M., Fry, D., and Chakrabarti, A. (2006). Aggregates, Superaggregates and Gel-Like Networks in Laminar Diffusion Flames, *J. Aerosol Science* 37:386-401.
- Kruk, M., and Jaroniec, M. (2001). Gas Adsorption Characterization of Ordered Organic-Inorganic Nanocomposite Materials, *Chem. Mater.* 13:3169-3183.
- Lushnikov, A. A., Negin, A. E., and Pakhomov, A. V. (1990). Experimental Observation of the Aerosol-Aerogel Transition, *Chem. Phys. Lett.* 175:138-142.
- MSDS (Material Safety Data Sheet) (1970). The Occupational Safety and Health Act of 1970.
- Palotas, A. B., Rainey, L. C., Sarofim, A. F., Vander Sande, J. B., and Ciambelli, P. (1996a). Effect of Oxidation on the Microstructure of Carbon Blacks, *Energy & Fuels* 10(1):254-259.
- Palotas, A. B., Rainey, L. C., Feldermann, C. J., Sarofim, A. F., and Vander Sande, J. B. (1996b). Soot Morphology: An Application of Image Analysis in High-Resolution Transmission Electron Microscopy, *Microscopy Research and Technique* 33(3):266-278.
- Palotas, A. B., Rainey, L. C., Sarofim, A. F., Vander Sande, J. B., and Flagan, R. C. (1998). Where Did That Soot Come From? *Chemtech*. 28(7):24-30.
- Pekala, R. W., Mayer, S. T., Kaschmitter, J. L., and Kong, F. M. (1994). Carbon Aerogels: An Update on Structure, Properties, and Applications. In Y. A. Attia (ed.), *Sol-Gel Process. Appl.* (Proc. Int. Symp. Adv. Sol-Gel Process. Appl.), 369-377.
- Reynolds, G. A. M., Dresselhaus, M. S., and Pekala, R. W. (1996). A Brief Overview of Structure-Property Relations in Carbon Aerogels, *Proceedings-Electrochemical Society*, 96-10 (Recent Advances in the Chemistry and Physics of Fullerenes and Related Materials, Vol. 3), 740-748.
- Sorensen, C. M., Hageman, W. B., Rush, T. J., Huang, H., and Oh, C. (1998). Aerogelation in a Flame Soot Aerosol, *Phys. Rev. Lett.* 80:1782-1785.